PHILOSOPHICAL TRANSACTIONS B

royalsocietypublishing.org/journal/rstb

Research

Cite this article: McKnight JC *et al*. 2021 Shining new light on sensory brain activation and physiological measurement in seals using wearable optical technology. *Phil. Trans. R. Soc. B* **376**: 20200224.
https://doi.org/10.1098/rstb.2020.0224

Accepted: 23 November 2020

One contribution of 10 to a theme issue 'Measuring physiology in free-living animals (Part I)'.

Subject Areas:
physiology

Keywords:
functional near-infrared spectroscopy, near-infrared spectroscopy, seal, sensory ecology, brain activation

Author for correspondence:
J. Chris McKnight
e-mail: jcm20@st-andrews.ac.uk

Electronic supplementary material is available online at https://doi.org/10.6084/m9.figshare.c.5429375.

THE ROYAL SOCIETY PUBLISHING

Shining new light on sensory brain activation and physiological measurement in seals using wearable optical technology

J. Chris McKnight[1], Alexander Ruesch[3], Kimberley Bennett[4], Mathijs Bronkhorst[5], Steve Balfour[2], Simon E. W. Moss[1], Ryan Milne[1], Peter L. Tyack[1], Jana M. Kainerstorfer[3,6] and Gordon D. Hastie[1]

[1]Sea Mammal Research Unit, and [2]Sea Mammal Research Unit Instrumentation Group, Scottish Oceans Institute, University of St Andrews, St Andrews, UK
[3]Department of Biomedical Engineering, Carnegie Mellon University, 5000 Forbes Avenue, Pittsburgh, PA 15213, USA
[4]Division of Science, School of Engineering and Technology, Abertay University, Dundee, UK
[5]Artinis Medical Systems BV, Einsteinweg 17, 6662 PW Elst, The Netherlands
[6]Department of Biomedical Engineering, Carnegie Mellon University, 5000 Forbes Ave., Pittsburgh, PA 15213, USA

JCM, 0000-0002-3872-4886; KB, 0000-0003-2168-6112; MB, 0000-0002-0410-0303; PLT, 0000-0002-8409-4790; GDH, 0000-0002-9773-2755

Sensory ecology and physiology of free-ranging animals is challenging to study but underpins our understanding of decision-making in the wild. Existing non-invasive human biomedical technology offers tools that could be harnessed to address these challenges. Functional near-infrared spectroscopy (fNIRS), a wearable, non-invasive biomedical imaging technique measures oxy- and deoxyhaemoglobin concentration changes that can be used to detect localized neural activation in the brain. We tested the efficacy of fNIRS to detect cortical activation in grey seals (*Halichoerus grypus*) and identify regions of the cortex associated with different senses (vision, hearing and touch). The activation of specific cerebral areas in seals was detected by fNIRS in responses to light (vision), sound (hearing) and whisker stimulation (touch). Physiological parameters, including heart and breathing rate, were also extracted from the fNIRS signal, which allowed neural and physiological responses to be monitored simultaneously. This is, to our knowledge, the first time fNIRS has been used to detect cortical activation in a non-domesticated or laboratory animal. Because fNIRS is non-invasive and wearable, this study demonstrates its potential as a tool to quantitatively investigate sensory perception and brain function while simultaneously recording heart rate, tissue and arterial oxygen saturation of haemoglobin, perfusion changes and breathing rate in free-ranging animals.

This article is part of the theme issue 'Measuring physiology in free-living animals (Part I)'.

1. Introduction

Animals respond continually to diverse environmental stimuli (e.g. sound, sight and touch) [1–3] to make critical ecological decisions (e.g. communication, foraging). Extensive research has described behavioural responses to such stimuli [4–7]. For example, experiments demonstrate that domestic sheep can recognize their offspring at a distance using visual and acoustic cues, with olfaction providing a final check of identity at close range before allowing suckling [8]. Specific areas of a sheep's cerebral cortex are involved in facial recognition and there is a specialized mechanism to learn offspring odours immediately after birth [9]. However, understanding how most species detect and perceive external stimuli rarely integrates information from several senses. Instead, basic knowledge of the structure [10] and function [11] of individual sensory apparatus is used along with measurements of their relative sensitivity, detection capacity and threshold ranges [12–14]. For example, we know that

deep-diving seals have acute vision adapted for the deep ocean [12], they can hear well underwater [13] and their vibrissae can detect the wake of fishes [14]; but it is currently unclear which of these senses they use at different stages of prey detection, localization and capture.

Although animals can perform some tasks when experimentally restricted to only one sensory system [15], and some behavioural characteristics are suggestive of task-based dominance of a particular sensory pathway (e.g. changing bearing in response to prey-derived bioluminescence [16]), under natural conditions most behaviours are based on multimodal convergence of input from several senses [3]. In addition, information from different senses may change in importance relative to other senses depending on the context. Our understanding of which senses animals rely upon to complete tasks in the wild (such as locating prey or detecting and fleeing danger) is complicated by the fact that sensing occurs in a spatially, temporally and contextually heterogeneous environment, in which information masking and central attentional factors, such as a focus on finding prey or detecting a predator, can affect how even simple stimuli are detected and processed [17]. Given the complexity of natural environments and the dynamic interactions that free-ranging animals must process, it is important to measure sensory activation under naturalistic conditions. An ability to understand multisensory perception, specifically sensory cortical activation, synchronously with behaviour and physiological parameters such as heart rate, is key to understanding contextual decision-making in the wild.

Visual, auditory, mechanoreceptive and chemoreceptive stimuli evoke responses from different regions of the cortex of the mammalian brain [18]. The location of these areas varies across mammals, but the specialization of cortical areas for different senses is shared across mammals. If the areas of cortex activated by each sense are mapped in a species, then a method to detect activation of those regions in a free-ranging individual should identify which sense is activated during different behaviours.

Several methods are available for topographical mapping of cortical activation, but few are suitable to work with wild animals engaged in normal behaviour in their natural environments. Magnetoencephalography (MEG) and electroencephalography (EEG) can measure magnetic and electrical fields generated by neural activity with good temporal resolution, but MEG equipment is limited to the laboratory, which limits the species, contexts and environmental conditions that can be investigated. EEG signals from the brain can be overwhelmed by electrical signals from muscle tissue when animals are moving and behaving. Functional magnetic resonance imaging (fMRI) can measure localized changes in blood oxygenation due to increases in metabolic rate of activated tissue [19]. It has excellent spatial resolution, but MRI equipment is static and laboratory-based. Alternatively, functional near-infrared spectroscopy (fNIRS) uses the same changes in haemoglobin concentration to map brain activity [20], but is non-invasive, wearable and can potentially be ruggedized to collect physiological data on animals in extreme environments [21]. Therefore, fNIRS has the potential as a tool to study animal sensory biology through brain activation in free-ranging contexts.

The haemodynamic response (HR) to stimulation is the fundamental basis by which fMRI and fNIRS identify regions of activation within the brain. In humans, the HR is characterized by an increase in oxyhaemoglobin [HbO] of approximately 1.0 µM [22] and a moderate decrease in deoxyhaemoglobin [HbR], resulting in an increase in blood volume and blood oxygen concentration that supports increased neuronal metabolic demand in active brain regions, e.g. in the occipital cortex during a visual task. As cortical activation is proximally measured through haemodynamic and oxygenation changes, other physiological processes such as cardiac function, changes in vascular tone, respiration and changes in blood oxygen saturation are captured by fNIRS. Heart rate, respiration, tissue-specific perfusion changes, tissue-specific oxygenation changes, arterial blood oxygenation and blood pressure changes are all physiological signals available from raw fNIRS data [23]. While these physiological signals are generally accounted for and removed to determine the underlying cortical activation responses in neuroimaging studies, these signals are important in bioenergetics research [24] and for tracking physiological responses to environmental covariates and anthropogenic disturbance [25]. The combination of physiological and cortical activation data make fNIRS a potentially powerful tool, particularly if these measurements could be integrated into existing behavioural and environmental data logging platforms, to measure responses to external stimuli as animals interact with their environment in the wild.

Although fNIRS has been used in a small number of terrestrial, domestic species (such as sheep and dogs) in controlled laboratory settings [26–30], it has not, to our knowledge, been used to study the sensory biology of wild animals. This method will be particularly useful for species that are accessible for attachment of a biologging device, but, once released into their natural environment, perform important behaviours where they are no longer accessible for direct observation.

Here, we describe the application of fNIRS on grey seals (*Halichoerus grypus*) to map cortical activation associated with different sensory modalities. Specifically, using stimulation of three sensory modalities (vision, hearing and mechanoreception), we describe the topographical areas of regional activation and distinction between areas associated with each sense, the shape and timing of the cerebral HR indicative of activation, as well as systemic physiological parameters collected simultaneously by fNIRS. Our results have significant implications for the development of biologging tools to measure sensory responses of wild animals, and their integration with physiological and behavioural metrics to allow a better understanding of reactions to complex stimuli in the wild. We propose that fNIRS has potential not only for fundamental sensory ecology research but also to study the effects of potentially distracting stimuli from human activities and harmful objects such as fishing gear, which are of growing conservation concern.

2. Material and methods

(a) Subject details

Experiments were conducted with five temporarily captive juvenile grey seals (*H. grypus*) housed at the Sea Mammal Research Unit (SMRU), University of St Andrews. All animals were captured in the Moray Firth, Scotland, and transported to and temporarily housed at the SMRU animal facility; consisting of three unheated seawater pools. Animals were released to the wild following completion of the experiments.

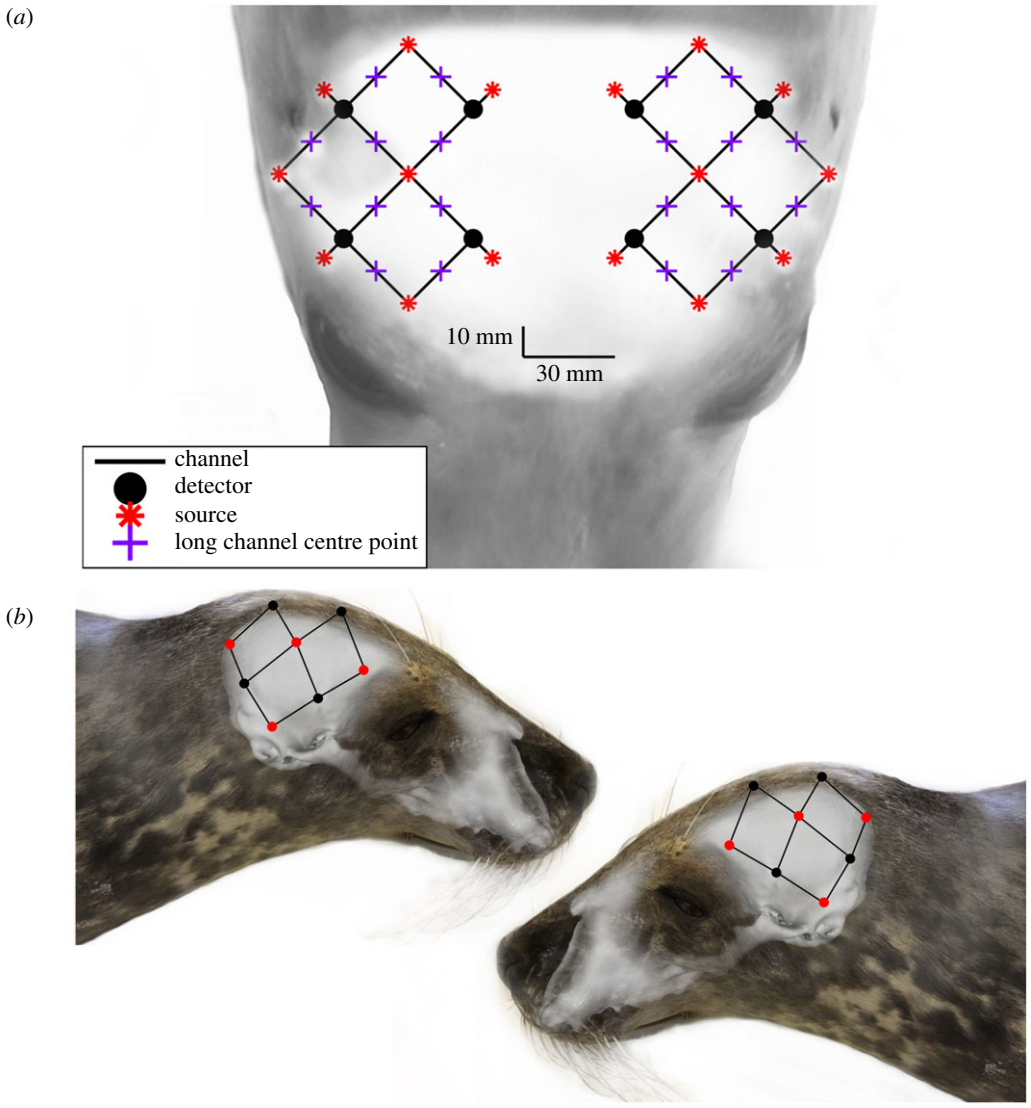

Figure 1. (*a*) The optode array configuration overlayed on the head of a seal for anatomical perspective. (*b*) The anatomically and spatially accurate location of the light sources (red points) and detectors (black points) overlayed on the skull of a juvenile grey seal. Black lines indicate each of twenty 3 cm optode–detector distance channels.

(b) Functional near-infrared spectroscopy instrumentation

Data were collected using a wearable NIRS device ('Brite24' Artinis Medical Systems BV, Einsteinweg, The Netherlands) with 16 dual-wavelength emitters and eight photodiode detectors, configured to provide 20 emitter–detector pairs (channels) (figure 1). The 16 LED emitters each had two NIR light sources with wavelengths of 760 and 850 nm, and the eight photodiode detectors had ambient light filters. Twenty channels had an optode–detector separation distance of approximately 30 mm. The system contained eight short (10 mm) channels that were not included in analysis.

(c) Optode attachment

A customized neoprene headcap was developed to fit the head of seals. Using three-dimensional photogrammetry software (Photomodeler Scanner 2016, Photomodeler Technologies, Vancouver, Canada), a three-dimensional computational model of a seal head was rendered from photographs of an anaesthetized juvenile grey seal and three-dimensional-printed ('Form 2' Formlabs Inc., Somerville, MA, USA) at 1 : 1 scale to tailor a customized neoprene headcap that ensured contact was maintained between the seals' head and the optodes/detectors. To consistently place the optode/detectors in comparable locations across individual seals, skull features were used. The centre of the cap was placed in line with the sagittal crest, and the back of the cap with the nuchal crest. The front of the cap was 2 cm caudal to the supraorbital vibrissae. Additionally, an approximately 10 mm diameter area of fur under each optode/detector was shaved to the skin. This ensured the repeatability of optode/detector location between trials and prevented fur from impeding NIR light propagation.

(d) Determining functional near-infrared spectroscopy optode locations

To identify the anatomical position of the fNIRS emitters and detectors over the skull of a juvenile grey seal, the neoprene headcap used in experiments was fitted to the head of a freshly dead juvenile grey seal using the same cap placement described above. The headcap was then removed and a series of 40 photographs were taken of the carcass using a Nikon D90 camera and 18–70 Nikon lens with the focal length set to 18 mm. Three-dimensional photogrammetry software (Photomodeler Scanner 2016) was used to generate a three-dimensional computational model of the seal head that included the optode/detector locations (model A). The tissue overlying the skull was then

removed to expose the braincase. The carcass was imaged a second time (40 photographs) and a second three-dimensional photogrammetry model was generated (model B). Both models had a root mean squared (RMS) error of less than 2.0 (arbitrary units defined by PHOTOMODELER), which is within the acceptable threshold of accuracy (RMS 0–5) recommended by PHOTOMODELER software [31]. Both models were exported from PHOTOMODELER as *.stl files and combined in the software package MESH LAB (Visual Computing Lab, Istituto di Scienza e Tecnologie dell' Informazione 'A. Faedo', Italy), using anatomical features (eyes, nose, vibrissae) to align them. The optode/detector positions on the skin (model A) were then matched to the underlying locations on the skull (model B). The area covered by the optode/detector array is shown in figure 1 and was presumed to be representative of the cohort of juvenile grey seals used in experiments.

(e) Sensory stimuli

Visual, auditory and tactile stimuli were selected to stimulate each sense independently. Visual stimuli consisted of the presence and absence of torchlight (50 lumens) manually shone into the eyes from a range of 30 cm. Auditory stimuli consisted of five different anthropogenic sounds (electronic supplementary material, figure S1); these were (i) pile driving (500 m), (ii) pile driving (40 km), (iii) an operational tidal turbine (low sound pressure level), (iv) an operational tidal turbine (high sound pressure level), and (v) a training whistle. Previous research has shown that acoustic characteristics (e.g. source level, rise time, signal duration, signal frequency) can have a significant influence on the probability of detection by an animal [29]. Therefore, by selecting a range of sounds with different acoustic characteristics, we hoped to maximize the probability of inducing an HR to the acoustic stimuli. The pile-driving signals were derived from two far-field measurements of pile driving (500 m and 40 km from the source) in a shallow water environment [30]. Similarly, the tidal turbine signal was generated to show comparative far-field temporal and spectral characteristics of real turbine noise [6]. The training whistle signal was a recording of a whistle used by training and husbandry personnel as a conditioned reinforcement 'bridging' signal [32] during feeding of the seals. The majority of the signals (pile driving (500 m), pile driving (40 km), the tidal turbine (low sound pressure level), and the training whistle were played at the same source sound pressure level (approx. 86.5 dB re 20 µPa @ 1 m (RMS)). A high sound pressure level tidal turbine signal was also played at approximately 94 dB re 20 µPa @ 1 m (RMS). Noise was kept to a minimum during the experimental trials with a resultant median ambient noise of 59.7 dB (95% confidence intervals: 55.7–64.4) re 20 µPa (electronic supplementary material, table S1). All sounds were combined for the analysis of auditory stimuli.

Signals were played from an HP Elitebook laptop computer using a speaker (MX Sound, Logitech, Lausanne, Switzerland) located approximately 1 m in front of the animal's head, in line with its longitudinal axis. Transducer calibrations were made using a calibrated mini-DSP UMIK-1 measurement microphone (frequency response: 14 Hz – 20 kHz ± 1 dB) and a laptop computer.

Tactile stimuli consisted of the presence and absence of manual stimulation of either the right or left mystacial and supraorbital vibrissae by gently stroking the whiskers.

(f) Experimental procedure

Approximately 10–15 min before sensory stimulus experiments, each seal was sedated using a combination of midazolam (Hypnovel, Roche Products Ltd, UK; 5 mg ml^{-1} solution, 0.03 ml kg^{-1} intramuscular) and ketamine (Ketaset, Zoetis, UK 100 mg ml^{-1} solution, 0.01 ml kg^{-1} intravenous). The seals were then moved to a table in a relatively quiet and evenly lit indoor laboratory. A respiratory band ('FLOW', Sweetzpot, Oslo, Norway) was placed around the chest to measure respiratory activity, allowing respiratory activity signals to be filtered from the NIRS data. The neoprene headcap was fitted on the seals head ensuring that optodes and detectors were located on the exposed skin. The signal on each channel was checked to ensure continuous cardiac pulsation was present in real-time raw data relay from the fNIRS instrument to a PC, before proceeding with experimental exposures.

The experiments consisted of three epochs (one for each sensory stimulus), each consisting of 8–10 blocks of stimulus presentation (electronic supplementary material, figure S2). Each block was 15 s in duration and was followed by 15 s of stimulus absence. Each epoch was preceded and followed by a 30 s period without stimulus. Epoch order was randomized and the order of the sounds presented and the vibrissal assemblage stimulated were randomized within epochs. The presentation of instructions for manual stimulation (visual and tactile stimulation) and presentation of auditory stimulation was controlled using E-PRIME 3.0, which also time-stamped each stimulus presentation to the fNIRS control software, OXYSOFT (v. 3.2.51.2, Artinis Medical Systems BV, Einsteinweg, The Netherlands). Timings associated with E-PRIME, OXYSOFT and the respiratory band were synchronized prior to each experiment. Each seal was exposed to the experimental procedure twice. Each experimental procedure was separated by 6 (four seals) or 7 (one seal) days. This experimental procedure was a balance between assessing as many stimuli as possible with the minimum amount of stimulus blocks expected to observe an HR, while minimizing animal handling time.

(g) Analysis of functional near-infrared spectroscopy

To extract the HR to evoked neuronal activation, we first manually reviewed trials and removed those that showed large-movement artefacts, sparse respiration events and detector saturation as determined by the fluctuation magnitude, rate of change and presence of vital signals like heart rate oscillations. For further functional analysis, the NIRS Brain AnalyzIR toolbox [33] was employed, in MATLAB (The MathWorks Inc., Natick, MA, USA). Firstly, a low-pass filter was applied to the data to reduce remaining signal noise from motion artefacts. Then, secondly, all data were trimmed to 30 s before the first stimulus to 30 s after the last stimulus. Thirdly, given the NIRS device had 20 channels across the probe, which equates to 40 measured time traces per animal per condition, processing the resultant 1160 time traces were computationally expensive; we, therefore, down-sampled the data from 10 to 5 Hz to increase the processing efficiency. However, it is important to highlight that, given the slow nature of an HR to neuronal activity, this reduction in sample rate did not affect the capacity to detect cortical activation. Raw intensity values were converted to optical density relative to the average intensity in the first 1% of the data. Remaining motion artefacts resulting in instantaneous intensity changes were removed by applying the temporal derivative distribution repair algorithm [34]. To remove global haemodynamic changes that are caused by systemic influences, such as respiration, heart rate or blood pressure changes, as well as for further motion artefact reduction, a principal component analysis filter was applied. Components of the largest eigenvalues were removed, such that no more than 70% of the variance in each measurement was removed. From here, the modified Beer–Lambert's law was applied, to calculate [ΔHbO], [ΔHbR] and change in total haemoglobin [ΔHbT]. Finally, a band-pass filter with a passband of 0.02–0.3 Hz was applied, using a fourth-order Butterworth filter.

To extract averaged HRs, a time window from 5 s before every stimulation onset to 35 s after the stimulation onset was extracted for each trial to represent pre-stimulation, stimulation and post-stimulation data. A two-sample *t*-test ('ttest2, MATLAB, The MathWorks Inc.) was used to establish the probability of a significant

increase in [ΔHbO] or decrease in [ΔHbR] of the signal after stimulation. For this analysis, 3 s of data before the stimulation onset were time-averaged for every stimulation presentation to provide a baseline distribution. Distributions for each 3 s period between 5 and 20 s after the stimulation onset were then compared to the baseline distribution to identify any statistical differences in pre- and post-stimulus concentrations of [ΔHbO] and [ΔHbR]. A measurement was considered to show a significant change from baseline if any one of the p-values between 5 and 20 s after stimulation onset showed $p < 0.05$.

Trials were then averaged per condition (auditory, visual, left tactile, right tactile stimulation) individually for all long-distance channels. In addition, Pearson's correlation ('corrcoef, MATLAB, The MathWorks Inc.) was calculated between [ΔHbO] and [ΔHbR] and used as a condition to distinguish HRs, with a negative correlation, from motion, with a positive correlation.

3. Results

The application here of fNIRS successfully measured the HR associated with cortical activation, during stimulation of three sensory pathways (vision, hearing and mechanoreception). Following data filtering, 43, 29 and 36 stimulus exposures for visual, auditory and tactile, respectively, were analysed for cortical activation detection. In addition to capturing cortical activation, fNIRS also collected high-resolution, continuous data on heart rate and breathing rate.

(a) Localized response to visual stimulation

Channels showing cortical activation during visual stimulation are shown in figure 2*a*. Five channels showed statistically significant group average changes in [HbO], indicative of bilateral cortical activation that occurred predominately in the posterior-medial region of the brain. The group-averaged mean changes in [HbO], [HbR] and [HbT] concentrations in response to a visual stimulus are shown in figure 2*b*. An increase in group-averaged mean (±s.e.) [HbO] in active channels were less than or equal to 0.1 µM. The HR was characterized by an overall increase in [HbO] during the period of activation, before declining following stimulus offset.

(b) Localized response to auditory stimulation

Channels showing cortical activation during auditory stimulation are shown in figure 3*a*. Six channels showed significant group average changes in [HbO] (figure 3*a*), distributed bilaterally extending anteriorly from the region of activation in the posterior of the brain during visual stimulation. The group-averaged mean changes in [HbO] and [HbR] concentrations in response to auditory stimuli are shown in figure 3*b*. An increase in group-averaged mean (±s.e.) [HbO] in active channels were less than or equal to 0.1 µM. HR was characterized by an overall increase in [HbO] following activation, declining during stimulation.

(c) Localized response to tactile stimulation

Channels showing cortical activation during tactile stimulation are shown in figure 4*a*. Four channels showed significant group-average changes in [HbO] (figures 4*a* and 5*a*). Three channels displayed activation during right vibrissal stimulation and one during left vibrissal stimulation. The group-averaged mean changes in [HbO] and [HbR] concentrations in response to vibrissal stimulation are depicted in figures 4 and 5*b*. An increase in group-averaged mean (±s.e.) [HbO] in active channels was less than or equal to 0.13 µ mol l^{-1}. HR was characterized by an increase in [HbO] during stimulation, followed by a decline either during stimulation or after stimulus offset.

(d) Systemic physiological signals

The haemodynamic consequences of cardiac function and respiration produced clear patterns in the raw fNIRS signals (figure 6). Blood volume changes with each cardiac cycle were visible as a cardiac waveform, with greater prominence in [ΔHbO] than [ΔHbR], providing a direct measure of heart rate. As shown in figure 6*a*, heart rate is apparent as clear peaks and troughs in the [ΔHbO] trace. As heart rate in a seal decreased, waveform peak (systolic peak) height increased, indicative of increasing blood pressure (figure 6*d*). Respiration events, which occurred sporadically (approx. every 40–60 s), resulted in significant oscillations in both [ΔHbO] and [ΔHbR] (figure 6*a*). Rapid, deep inspiration (positive peaks in figure 6*b*) caused a rapid increase in [ΔHbO] and a moderate decrease in [ΔHbR] which effectively masked the cardiac waveform. At the end of inspiration, and before breath-holding, animals contracted the thorax (figure 6*b*) which was maintained throughout the remainder of the breath-hold period. Coincident with this thoracic contraction was pronounced bradycardia (as seen in figure 6*a* in the time-series immediately before the black box—where frequency of cardiac pulsations are lower and cardiac pulsation height is greater), with an increase in [ΔHbO] and a decrease in [ΔHbR]. Seconds after the onset of bradycardia, [ΔHbO] decreased, [ΔHbR] increased and heart rate increased to a steady rate. On release of the breath-hold, expiration resulted in a rapid decrease in [ΔHbO] and an increase in [ΔHbR].

4. Discussion

The results presented here demonstrate that cortical haemodynamic alterations in response to sensory stimuli can be measured with fNIRS in a grey seal. Further, the HRs to each stimulus type can be localized and distinguished topographically. These results, together with simultaneous measurement of systemic cardiovascular changes (i.e. heart rate and breathing events), show that fNIRS has the potential to be an important tool for measuring sensory processing and physiological responses of free-ranging animals.

(a) Haemodynamic response shape

The shape of the HR in seals, for visual, acoustic and tactile stimulation (figures 2–5), was comparable to the HR in humans in the dynamics of both [HbO] and [HbR] but was lower in magnitude. The HR in humans is approximately 1.0 µM [22], while HR here in seals was less than or equal to 0.1 µM. Therefore, existing fNIRS data-processing protocols (and presumably fMRI) for humans can effectively capture visual, auditory and tactile sensory brain activation in seals.

(b) Visual stimulation

The visual cortex of almost all mammals is located in the posterior region of the cerebral cortex [18]. Results from the current study showed bilateral regional activation during visual stimulation also occurred in the posterior region of the

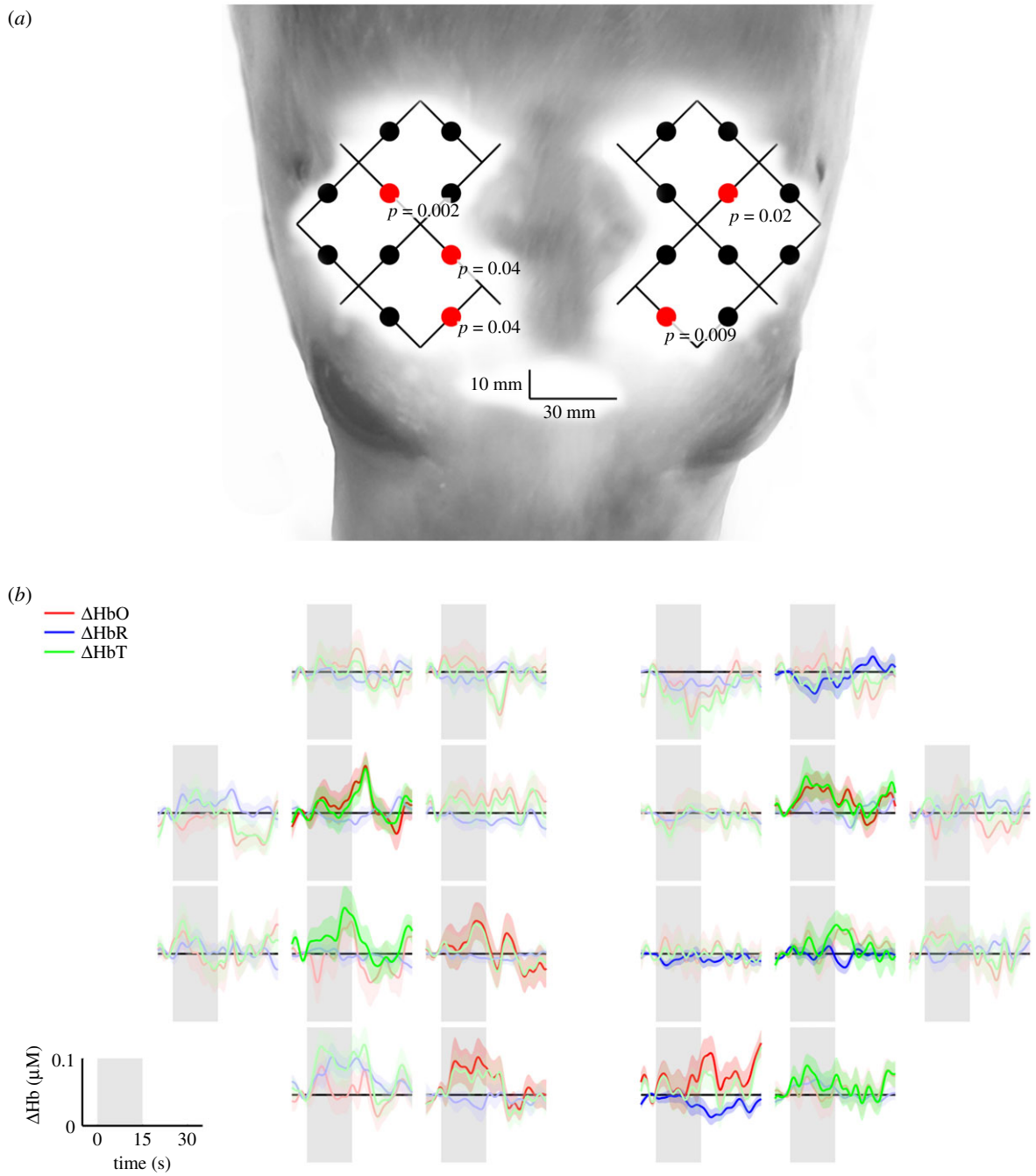

Figure 2. (*a*) Channels displaying statistically significant ($p < 0.05$) group average [HbO] changes during visual stimulation are indicated by red dots. The optical array is visualized over the head of a juvenile grey seal to show the anatomical perspective of regional activation. (*b*) Corresponding group average (lines) and standard error (ribbons) changes in [HbO], [HbR] and [HbT] over 15 s of visual stimulation (shaded grey area) followed by 15 s of no visual stimulation (white area). Bold colours represent a significant ($p < 0.05$) change in [HbO] and where [HbO] and [HbR] were negatively correlated.

brain (figure 6); this suggests that regional cortical activation in grey seals is consistent with that of other Carnivora, including the domestic dog (*Canis familiaris*) [35–37].

It also confirms predictions of the location of the primary visual cortex of northern elephant seals (*Mirounga angustirostris*) [38] and harp seals (*Pagophilus groenlandicus*) [39] from histological and cytoarchitectural markers on brain samples. These previous studies [38,39] predicted the primary visual cortex to overlap with the arrangement of the four most posterior and medial channels in figure 2*a*. The posterior-medial topographical organization of the seal visual cortex is also in agreement with visual evoked responses measured in Weddell seals (*Leptonychotes weddellii*) [40].

It is important to highlight that, during visual stimulation in the current study, seals contracted their pupil and directed the pupil towards the light source which would involve motor cortex function. The observed activation that occurred rostral to the visual cortex could, therefore, be related to motor cortex activation [41]. Previous work on harbour seals showing that cortical activation can be associated with the motor cortex [42] is also consistent with the rostral topographical activation during visual stimulation in the present study.

(c) Auditory stimulation

The auditory cortex of most mammals is located caudal, ventral or ventrocaudal to the Sylvian fissure [18]. The lateral arrangement of the auditory cortex in mammals is most often in close proximity to the posterior visual cortex [18]. Other carnivores

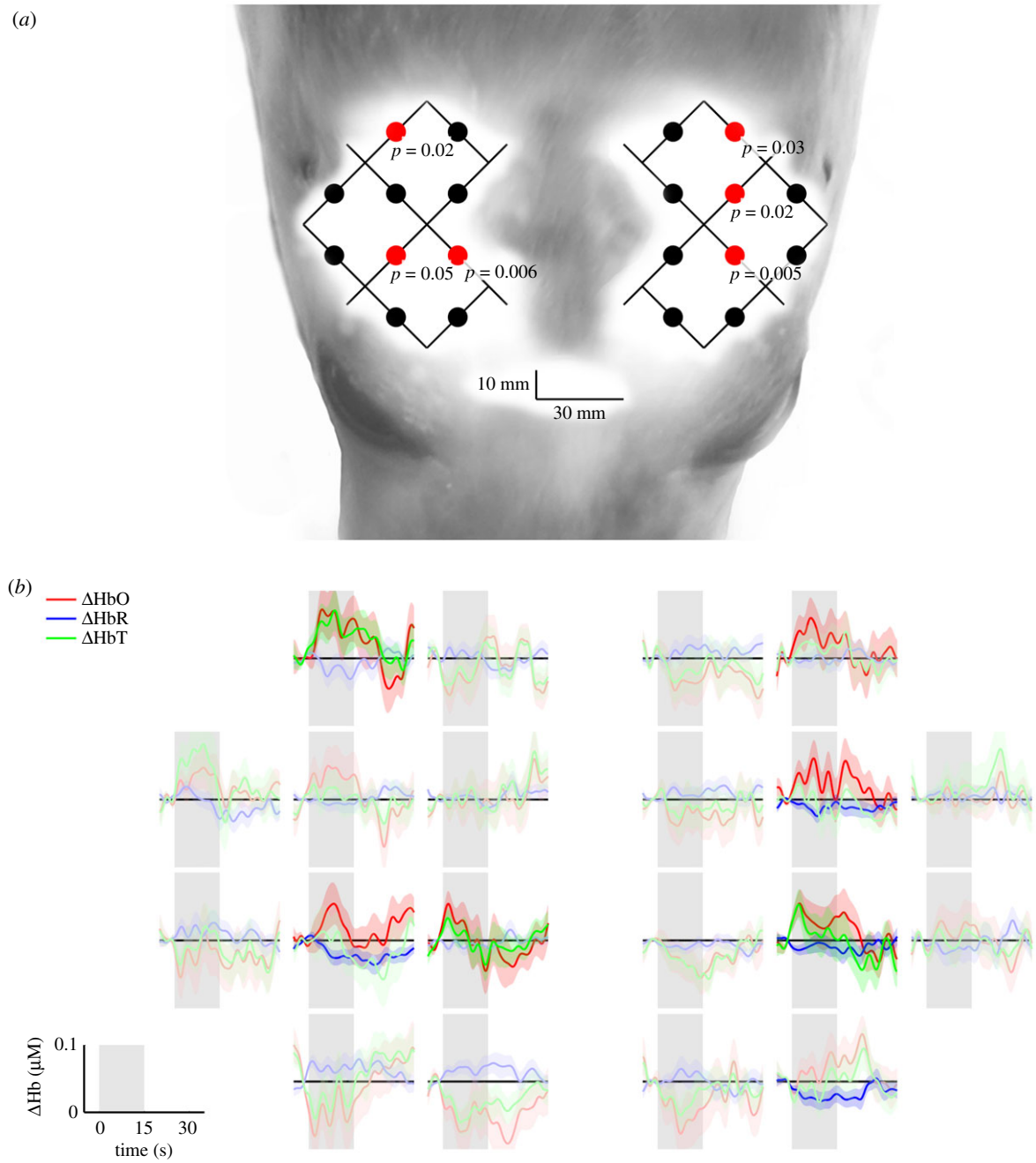

Figure 3. (*a*) Channels displaying statistically significant ($p < 0.05$) group average [HbO] changes during auditory stimulation are indicated by red dots. The optical array is visualized over the head of a juvenile grey seal to provide anatomical perspective of regional activation. (*b*) Corresponding group average (lines) and standard error (ribbons) changes in [HbO], [HbR] and [HbT] over 15 s of auditory stimulation (shaded grey area) followed by 15 s of no auditory stimulation (white area). Strong colours represent a significant ($p < 0.05$) change in [HbO] and where [HbO] and [HbR] were negatively correlated.

also display auditory activation ventral to the supra-Sylvian sulcus [43,44]. However, cortical activation during auditory stimulation in harbour seals has been reported more ventrally [45]. Cortical responses to auditory stimulation in the current study showed HRs, particularly in the three anteriorly active channels, that are consistent with topographical organization of the auditory cortex reported by Alderson *et al*. [45]. The activation to auditory stimulation extended posteriorly into the presumed visual cortex; this may have been a consequence of the seals attempting to visually locate the sound source during playbacks.

(d) Tactile stimulation

The location of the somatosensory cortex appears variable across mammals [18]. However, in most cases, the primary somatosensory cortex is located dorsorostrally to the auditory cortex, and the secondary somatosensory cortex is located in close proximity and rostral to the auditory cortex [18]. In the current study, vibrissal stimulation resulted in predominantly contralateral activation of the cortex and is consistent with previous measurements in northern fur seals (*Callorhinus ursinus*) [46] and other carnivores, such as dogs [18].

During right vibrissal stimulation, there was activation predominantly in the right cortex, with a topographical organization consistent with Ladygina *et al*. [46]. There was additional activation frontal activation in the left cortex. During left vibrissal stimulation, there was a single channel showing activation in the left cortex. The channel showing activation, while contralateral to the side of vibrissal stimulation, was caudal to the expected region of activation. There were, however, non-significant HRs in the channel

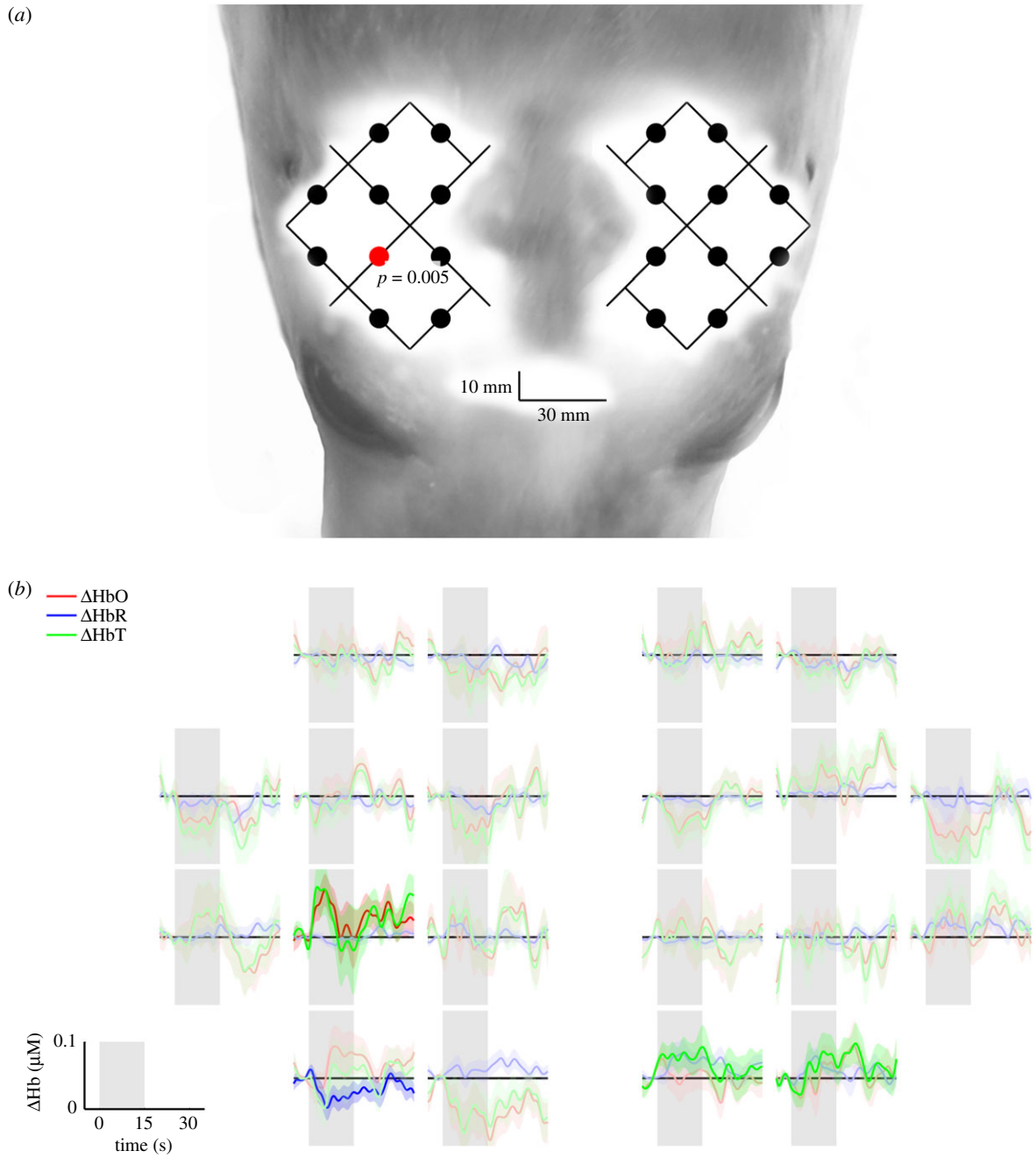

Figure 4. (*a*) Channels displaying statistically significant ($p < 0.05$) group average [HbO] changes during right vibrissal stimulation are indicated by red dots. The optical array is visualized over the head of a juvenile grey seal to provide anatomical perspective of regional activation. (*b*) Corresponding group average (lines) and standard error (ribbons) changes in [HbO], [HbR] and [HbT] over 15 s of right vibrissal stimulation (shaded grey area) followed by 15 s of no left vibrissal stimulation (white area). Strong colours represent a significant ($p < 0.05$) change in [HbO] and where [HbO] and [HbR] were negatively correlated.

anterior to the significant activation that would be consistent with right vibrissal stimulation and Ladygina *et al*. [46].

(e) Physiological monitoring

As we have demonstrated, the changes of [HbO] and [HbR] concentrations measured by fNIRS that allow cortical activation to be detected also contain a series of important systemic physiological signals such as respiration and cardiovascular function. While physiological signals like heartbeats and respiration tended to show a high signal-to-noise ratio in NIRS data, for functional imaging, these signals are considered artefacts owing to their relatively high signal strength in comparison to functional activation. In humans, where heart rate and respiration are relatively constant in frequency, a frequency-based filter can be used to remove these influences. In seals, the respiration events are intermittent, and heart rate and cerebral blood volume are modulated by respiration; this makes the removal of physiological signals uniquely challenging. For human fNIRS data, numerous methods exist to remove such physiological artefacts from the signal [47,48]. Some of these methods, including general linear models [49], will benefit from the establishment of a species-specific HR function (HRF), which is the mathematical description of the relationship between neuronal activation and HR or even the shape and duration of the HR itself. Although respiration induced the greatest magnitude of physiological contamination, it is important to highlight that seals in the wild spend approximately 80% of their time underwater [50]; the contamination owing to respiration observed in the current study is, therefore, likely to be significantly less in wild seals.

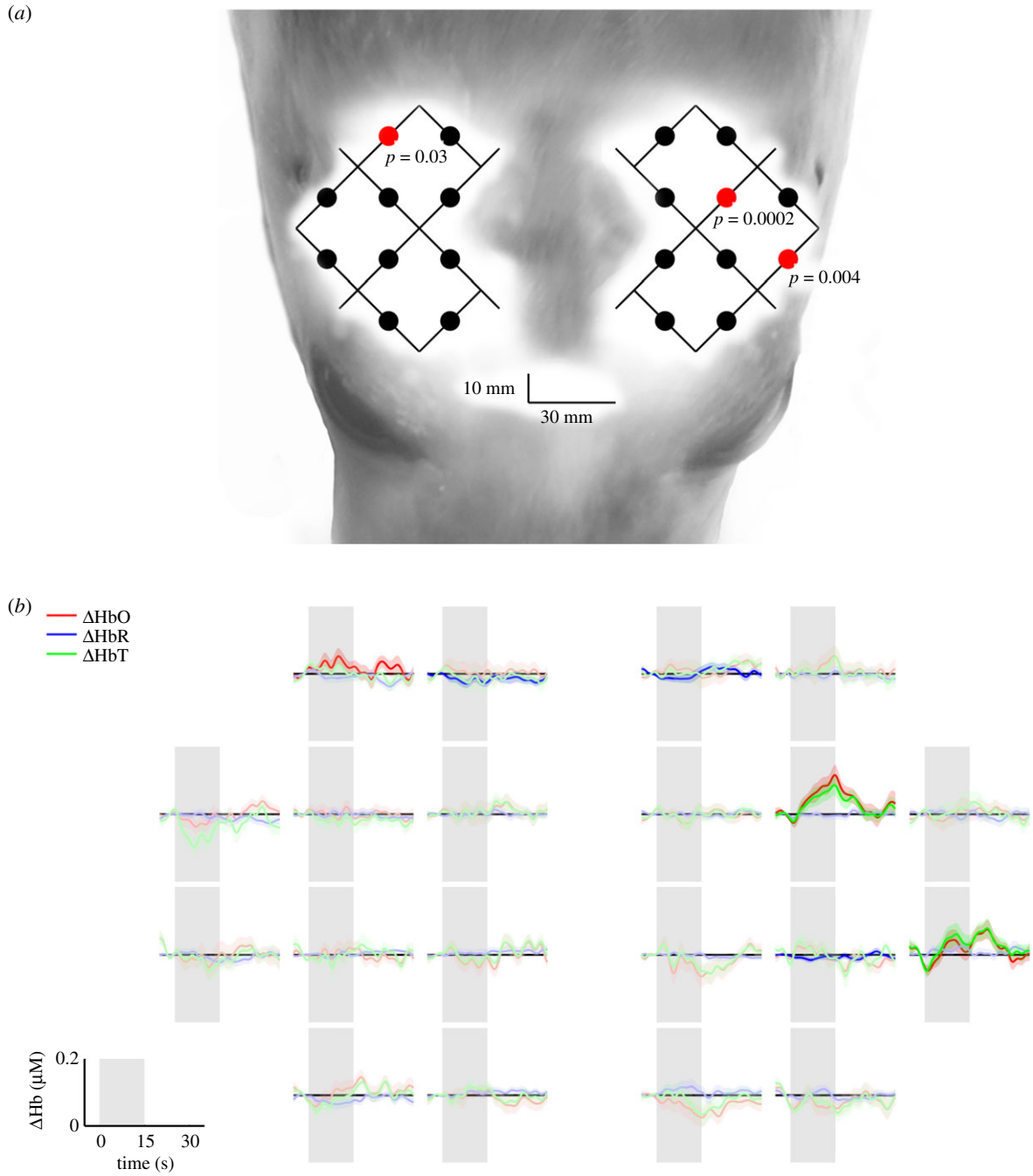

Figure 5. (*a*) Channels displaying statistically significant ($p < 0.05$) group average [HbO] changes during left vibrissal stimulation are indicated by red dots. The optical array is visualized over the head of a juvenile grey seal to provide anatomical perspective of regional activation. (*b*) Corresponding group average (lines) and standard error (ribbons) changes in [HbO], [HbR] and [HbT] over 15 s of left vibrissal stimulation (shaded grey area) followed by 15 s of no right vibrissal stimulation (white area). Strong colours represent a significant ($p < 0.05$) change in [HbO] and where [HbO] and [HbR] were negatively correlated.

Measuring heart rate through haemoglobin concentration fluctuations also provides information on cardiac waveform, which can provide information such as proxies for changes in blood pressure and potentially proxies for changes in intracranial pressure dynamics [51]. Further, analysis of both [HbO] and [HbR] cardiac waveforms can be used to calculate percentage arterial blood oxygen saturation [52] as recently employed to estimate SpO_2 in deep freediving humans [53]. Changes in [HbO] and [HbR] also provide measures of relative blood volume and tissue-specific blood oxygenation [21]. Finally, as a result of blood pressure changes due to intrathoracic pressure variation engendered by respiratory mechanics similar to the four stages of a Valsalva manoeuvre, [HbO] and [HbR] fluctuations with each exhalation, inhalation and apnoea can be used to identify individual breaths, as confirmed through the respiratory band data in the current study.

(f) Functional near-infrared spectroscopy in wild animals

This study represents an important first step in developing a biologging tool to measure sensory biology, through cortical activation in wild animals using non-invasive, wearable technology. Measuring sensory-specific regional activation with fNIRS provides a fundamental basis for understanding behavioural decision-making and behavioural interactions (such as locating prey or avoiding predators). Currently, our understanding of how wild animals interpret environmental

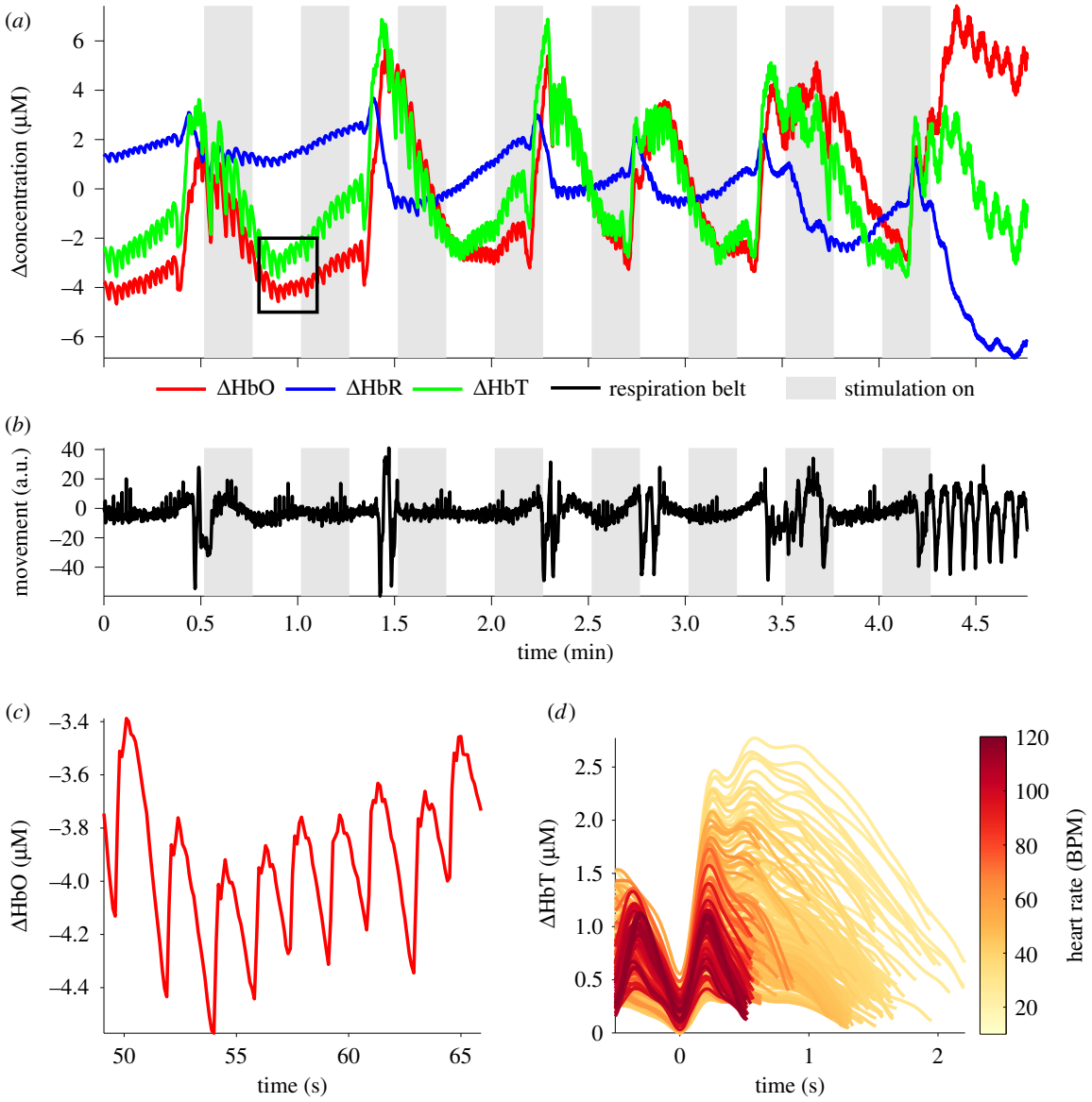

Figure 6. (*a*) Example of the raw [HbO] (red line), [HbR] (blue line) and [HbT] (green line) traces from a seal during the study, showing pulsatile cardiac waveform (for black box, see (*c*)) and dynamics associated with respiration. (*b*) Signal from the respiration band where the magnitude is directly correlated to chest movement. (*c*) Cardiac pulsation in [HbO] magnified from the black box in (*a*). (*d*) Cardiac pulsation of ΔHbT in a grey seal. Colour encodes the underlying heart rate (beats min^{-1}), beginning at diastolic minima at 0 s and ending at the next diastolic minima, revealing increasing pulse magnitude with lowering heart rates.

stimuli is largely hypothetical. We have demonstrated that fNIRS can detect patterns of haemodynamic change associated with cortical activation by sensory stimuli in seals. The topographical organization of cortical regions associated with visual, auditory, and tactile processing can be differentiated, although some overlap between regional activation does exist. This should allow perception through these three senses to be explored simultaneously and measure their relative importance under different ecological scenarios, such as foraging or predator avoidance.

From an applied perspective, measuring patterns of sensory activation with fNIRS may also offer important new perspectives in studies of the effects of potentially distracting or harmful stimuli from anthropogenic activities. For example, underwater sound from offshore industrial activities has been shown to elicit behavioural responses leading to avoidance in seals [6,54]. However, responses by animals appear to be highly context-specific [55] such that behavioural responses (or lack thereof) may be mediated by attentional factors, such as whether an animal is already engaged in an important activity such as foraging, which involves other senses that affect sound detection or decisions in how they respond. fNIRS could potentially allow an understanding of the underlying mechanisms and priority stimuli that contribute to decision-making, particularly when behavioural responses are potentially costly.

(g) Development considerations for an animal-borne functional near-infrared spectroscopy logger

The integration of fNIRS cortical activation data and the associated physiological data into existing behavioural and environmental data logging platforms [7,54] could provide a powerful suite of instantaneous and continuous measures of responses to external stimuli as animals interact with their environment in the wild. However, the current study was carried out on animals under controlled conditions, and there are a series of additional translational steps required before free-ranging animal studies are feasible.

(i) In the current study, senses were stimulated independently from others, whereas in the wild, it is

unlikely that animals will rely on only one sense at any one-time during events such as prey capture. Therefore, an important progression would be to conduct experiments that present combinations of single-sensory and multi-sensory stimulation to assess the capacity of fNIRS and to identify which senses are in use and potential time-dependent sensory dominance.

(ii) The results presented here were to a series of playbacks and sensory stimulations in air. For aquatic species such as seals, it would be useful to repeat these underwater to confirm that the patterns of activation are consistent across mediums.

(iii) Measuring NIRS signals in mobile subjects is significantly more challenging owing to the influence of factors such as motion artefacts [47]. Therefore, efforts to study mobile animals in managed or controlled conditions would be an advisable next step. Reducing/managing impact of motion artefacts could be addressed either mechanically, through appropriate optode/receiver attachment, or computationally, through signal processing. In humans, motion artefacts are easily generated through head movements that cause decoupling between optode/detectors and the scalp. The use of headcaps in human fNIRS research that cradle and locate the optode/detectors could be improved upon in animal research to generate more robust, continual contact between hardware and the scalp that is less sensitive to body movement. Alternatively, the use of adhesives for instrument attachment is routine in animals such as seals and are likely to reduce motion artefacts issues that impact human fNIRS research by providing more reliable hardware/skin contact. Furthermore, a range of available fNIRS motion artefact detection and correction approaches could be applied here [47]. These approaches, some of which could use existing animal-borne technology such as accelerometers [56], could be helpful for recovering usable fNIRS signals in mobile animals.

(iv) While the current study demonstrates the efficacy and use of fNIRS in a single species, there are important considerations for its future development and application across species. For example, from a neuroimaging perspective, substantial work has been conducted on humans to facilitate translation of signals derived from the scalp to the brain. However, the accuracy of topographical projections of cortical activation signals is currently relatively limited for new species. To ensure fNIRS can be applied to new animal models, accurate topographical projections of animals with fundamentally different skull shapes, skull thicknesses, extracranial anatomical differences and gross physiological differences would probably be required. This is required to ensure that optode array placements in relation to skull morphological features can be standardized and allow meaningful comparisons between species, and age-classes. Collaboration with anatomists and neuroanatomists may be of great importance in the future if independent studies with fNIRS are to be comparable and more accurate. Alternatively, neuroanatomical tools such as MRI (where feasible) would potentially help to understand the regions of the brain interrogated with the fNIRS optical path.

(v) Another important precursor to using fNIRS in any new species is the accurate measurement of the optical properties of different tissues (skin, muscle, fat, skull, blood, brain) as these may affect the penetration of the existing wavelengths in commercial fNIRS systems and may inform optimal alternate wavelengths required. Coupling optical property measurements with three-dimensional Monte Carlo simulations [57] would provide more accurate estimation of where in the brain, the activation is being measured. In the current study, we used commercially available wavelengths suitable for humans, because seal haemoglobin has similar optical properties to humans [58], there is a short distance from scalp to brain (less than 1.5 cm—typically less than a human), and fNIRS has been successfully used on seals to measure blood volume in the brain and blubber [21]. However, for species without this information, the absorption and scattering coefficients should be measured, and the dynamics of optical propagation estimated.

(vi) In terms of the physical deployment of an fNIRS logger on an animal, it is important that this is not only robust but does not unduly influence the behaviour or energetics of the animal [59]. Appropriate ruggedization/marinization while maintaining optical-integrity and appropriate attachment protocols is, therefore, required to allow fNIRS to be used on wild animals. Initial work on seals [21] and deep-diving humans [53], although restricted to single-channel systems, has shown that this is readily achievable even for extreme environmental conditions.

5. Conclusion

We have shown fNIRS can be used to measure sensory activation, along with simultaneous measurement of systemic cardiovascular changes (i.e. heart rate and breathing events) in seals, and demonstrate that its powerful applications in human biomedical and cognitive research could translate to free-ranging wild animal research. The capacity of fNIRS to simultaneously capture cortical activation and systemic physiological responses in a non-invasive, wearable instrument may facilitate free-ranging measurements. Together with data from existing animal-borne behavioural and environmental data logging systems, such data could provide key information to understanding sensory perception, behavioural responses and decision-making in wild animals.

Ethics. Procedures for capture, handling and housing of animals conformed to the Animals (Scientific Procedures) Act 1986, under the Sea Mammal Research Units' Home Office licence (no. 70/7806) and were performed by personnel deemed competent under EU directive of the protection of animals used for scientific purposes.

Data accessibility. This article has no additional data.

Authors' contributions. J.C.M., G.D.H., K.B. and P.L.T. conceived the study. J.C.M., G.D.H., S.E.W.M. and R.M. performed experiments. M.B. and S.B. provided technical assistance in the development of the fNIRS system. A.R., J.K. and J.C.M. provided model code and results. J.C.M. wrote the manuscript. G.D.H., J.K., G.D.H., P.L.T. and K.B. contributed to the writing of the manuscript and all authors provided comments. G.D.H. and J.K. provided equal project supervision and co-last authorship.

Competing interests. We declare we have no competing interests

Funding. This project was funded as part of the Department for Business, Energy and Industrial Strategy Offshore Energy Strategic Environmental Assessment Programme. Supplementary funding supporting J.C.M. and P.L.T. was provided by the US Office of Naval Research (ONR) grant nos N00014-18-1-2062 and N00014-20-1-2709.

Supplementary funding supporting J.K. and A.R. was provided by the US Office of Naval Research (ONR) grant no. N00014-19-1-1223. Assistance in funding for acquisition of the fNIRS system was provided by SMRU Consulting's 10th Anniversary Award.

References

1. Thompson D, Fedak MA. 2001 How long should a dive last? A simple model of foraging decisions by breath-hold divers in a patchy environment. *Anim. Behav.* **61**, 287–296. (doi:10.1006/anbe.2000.1539)
2. Sparling CE, Georges J-Y, Gallon SL, Fedak M, Thompson D. 2007 How long does a dive last? Foraging decisions by breath-hold divers in a patchy environment: a test of a simple model. *Anim. Behav.* **74**, 207–218. (doi:10.1016/j.anbehav.2006.06.022)
3. Hanke W, Dehnhardt G. 2013 Sensory biology of aquatic mammals. *J. Comp. Physiol. A* **199**, 417. (doi:10.1007/s00359-013-0823-9)
4. Cox TM *et al.* 2006 Understanding the impacts of anthropogenic sound on beaked whales. *J. Cetac. Res. Manage.* **7**, 177–187.
5. Slabbekoorn H, Bouton N, Van Opzeeland I, Coers A, ten Cate C, Popper AN. 2010 A noisy spring: the impact of globally rising underwater sound levels on fish. *Trends Ecol. Evol.* **27**, 419–427. (doi:10.1016/j.tree.2010.04.005)
6. Hastie GD, Russell DJF, Lepper P, Elliott J, Wilson B, Benjamins S, Thompson D. 2017 Harbour seals avoid tidal turbine noise: implications for collision risk. *J. Appl. Ecol.* **55**, 684–693. (doi:10.1111/1365-2664.12981)
7. Mikkelsen L, Johnson M, Wisniewska DM, van Neer A, Siebert U, Madsen T, Teilmann J. 2019 Long-term sound and movement recording tags to study natural behaviour and reaction to ship noise of seals. *Ecol. Evol.* **9**, 2588–2601. (doi:10.1002/ece3.4923)
8. Searby A, Jouventin P. 2003 Mother-lamb acoustic recognition in sheep: a frequency coding. *Proc. R. Soc. Lond. B* **270**, 1765–1771. (doi:10.1098/rspb.2003.2442)
9. Kendrick KM. 1994 Neurobiological correlates of visual and olfactory recognition in sheep. *Behav. Process.* **33**, 89–111. (doi:10.1016/0376-6357(94)90061-2)
10. Hanke FD, Dehnhardt G, Schaeffel F, Hanke W. 2006 Corneal topography, refractive state, and accommodation in harbour seals (*Phoca vitulina*). *Vis. Res.* **46**, 837–847. (doi:10.1016/j.visres.2005.09.019)
11. Dykes RW. 1975 Afferent fibres from mystacial vibrissae of cats and seals. *J. Neurophysiol.* **38**, 650–662. (doi:10.1152/jn.1975.38.3.650)
12. Hanke FD, Hanke W, Scholtyssek C, Dahnhardt G. 2009 Basic mechanisms in pinniped vision. *Exp. Brain Res.* **199**, 299. (doi:10.1007/s00221-009-1793-6)
13. Reichmuth C, Holt MM, Mulsow J, Sills JM, Southall BL. 2013 Comparative assessment of amphibious hearing in pinnipeds. *J. Comp. Physiol. A* **199**, 491. (doi:10.1007/s00359-013-0813-y)
14. Wieskotten S, Mauck B, Miersch L, Dehnhardt G, Hanke W. 2011 Hydrodynamic discrimination of wakes caused by objects of different size and shape in a harbour seal (*Phoca vitulina*). *J. Exp. Biol.* **214**, 1922–1930. (doi:10.1242/jeb.053926)
15. Gläser N, Wieskotten S, Otter C, Dehnhardt G, Hanke W. 2011 Hydrodynamic trail following in a California sea lion (*Zalophus californianus*). *J. Comp. Physiol. A* **197**, 141–151. (doi:10.1007/s00359-010-0594-5)
16. Vacquié-Garcia J, Mallefet J, Ballieul F, Picard B, Guinet C. 2017 Marine bioluminescence: measurement by a classical light sensor and related foraging behaviour of a deep diving predator. *J. Photochem. Photobiol. B* **93**, 1312–1319. (doi:10.1111/php.12776)
17. Durlach NI, Mason CR, Kidd G, Arbogast TL, Colburn HS, Shinn-Cunningham BG. 2003 Note on informational masking (L). *J. Acout. Soc. Am.* **113**, 2984. (doi:10.1121/1.1570435)
18. Johnson JI. 1990 Comparative development of somatic sensory cortex. In *Cerebral cortex*, vol. 8B (eds EG Jones, A Peters), pp. 335–449. Boston, MA: Springer.
19. Strangman G, Culver JP, Thompson JH, Boas DA. 2002 A quantitative comparison of simultaneous BOLD fMRI and NIRS recordings during functional brain activation. *Neuroimage* **17**, 719–731. (doi:10.1006/nimg.2002.1227)
20. Ferrari M, Quaresima V. 2012 A brief review on the history of human functional near-infrared spectroscopy (fNIRS) development and fields of application. *Neuroimage* **63**, 921–935. (doi:10.1016/j.neuroimage.2012.03.049)
21. McKnight JC *et al.* 2019 Shining new light on mammalian diving physiology using wearable near-infrared spectroscopy. *PLoS Biol.* **17**, e3000306. (doi:10.1371/journal.pbio.3000306)
22. Boas DA, Gaudette T, Strangman G, Cheng X, Marota JJA, Mandeville JB. 2001 The accuracy of near infrared spectroscopy and imaging during focal changes in cerebral hemodynamics. *Neuroimage* **13**, 76–90. (doi:10.1006/nimg.2000.0674)
23. Pinti P, Scholkmann F, Hamilton A, Burgess P, Tachtsidis I. 2019 Current status and issues regarding pre-processing of fNIRS neuroimaging data: an investigation of diverse signal filtering methods within a general linear model framework. *Front. Hum. Neurosci.* **12**, 505. (doi:10.3389/fnhum.2018.00505)
24. Butler PJ, Green GA, Boyd IL, Speakman JR. 2004 Measuring metabolic rate in the field: the pros and cons of the doubly labelled water and heart rate methods. *Funct. Ecol.* **18**, 163–183. (doi:10.1111/j.0269-8463.2004.00821.x)
25. Williams TM, Blackwell SB, Richter B, Sinding M-HS, Heide-Jørgensen MP. 2017 Paradoxical escape responses by narwhals (*Monodon monoceros*). *Science* **358**, 1321–1331. (doi:10.1126/science.aao2740)
26. Gygax L, Reefman N, Pilheden T, Scholkmann F, Keeling L. 2015 Dog behaviour but not frontal reaction changes in repeated positive interactions with a human: a non-invasive pilot study using functional near-infrared spectroscopy (fNIRS). *Behav. Brain Res.* **281**, 172–176. (doi:10.1016/j.bbr.2014.11.044)
27. Kawaguchi H, Higo N, Kato J, Matsuda K, Yamada T. 2017 Functional near infrared spectroscopy for awake monkey to accelerate neurorehabilitation study. In *Proc. SPIE 10051, Neural Imaging and Q2 Sensing*, 1005117, 8 February 2017, San Francisco, CA, USA.
28. Chincarini M *et al.* 2019 Evaluation of sheep anticipatory response to a food reward by means of functional near-infrared spectroscopy. *Animals* **9**, 11. (doi:10.3390/ani9010011)
29. Kastelein RA, Hoek L, Wensveen PJ, Terhune JM. 2010 The effect of signal duration on the underwater hearing thresholds of two harbor seals (*Phoca vitulina*) for single tonal signals between 0.2 and 40 kHz. *J. Acoust. Soc. Am.* **127**, 1135–1145. (doi:10.1121/1.3283019)
30. Hastie GD, Merchant ND, Götz T, Russell DJF, Thompson P, Janik VM. 2019 Effects of impulsive noise on marine mammals: investigating range-dependent risk. *Ecol. Appl.* **29**, e01906. (doi:10.1002/eap.1906)
31. De Bruyn PJN, Bester MN, Carlini AR, Oosthuizen WC. 2009 How to weigh an elephant seal with one finger: a simple three-dimensional photogrammetric application. *Aquat. Biol.* **5**, 31–39. (doi:10.3354/ab00135).
32. Heindenreich B. 2007 An introduction to positive reinforcement training and its benefits. *J. Exot. Pet. Med.* **16**, 19–23. (doi:10.1053/j.jepm.2006.11.005)
33. Santosa H, Zhai X, Fishburn F, Huppert T. 2018 The NIRS Brain AnalyzIR toolbox. *Algorithms* **11**, 73. (doi:10.3390/A11050073)
34. Fishburn FA, Ludlum RS, Vaidya CJ, Medvedev AV. 2019 Temporal derivative distribution repair (TDDR): a motion correction method for fNIRS. *Neuroimage* **184**, 171–179. (doi:10.1016/j.neuroimage.2018.09.025)
35. Dilks DD, Cook P, Weiller SK, Berns HP, Spivak M, Berns GS. 2015 Awake fMRI reveals a specialized region in dog temporal cortex for face processing. *PeerJ* **3**, e1115. (doi:10.7717/peerj.1115)
36. Berns GS, Brooks AM, Spivak M, Levy K. 2017 Functional MRI in awake dogs predicts suitability for assistance work. *Sci. Rep.* **7**, 43704. (doi:10.1101/080325)
37. Thompkins AM, Ramaiahgari B, Zhao S, Gotoor SSR, Waggoner TS, Deshpande G, Katz JS. 2018 Separate

brain areas for processing human and dog faces as revealed by awake fMRI in dogs (*Canis familiaris*). *Learn. Behav.* **46**, 561–573. (doi:10.3758/s13420-018-0352-z)

38. Turner EC, Sawyer EK, Kaas JH. 2017 Optic nerve, superior colliculus, visual thalamus, and primary visual cortex of the northern elephant seal (*Mirounga angustirostris*) and California sea lion (*Zalophus californianus*). *J. Comp. Neurol.* **525**, 2109–2132. (doi:10.1002/cne.24188)
39. Walloe S, Eriksen N, Dabelsteen T, Pakkenberg B. 2010 A neurological comparative study of the harp seal (*Pagophilus groenlandicus*) and harbor porpoise (*Phocoena phocoena*) brain. *Anat. Rec.* **293**, 2129–2135. (doi:10.1002/ar.21295)
40. Gruenau SP, Shurley JT. 1976 Visual evoked response (VER) changes during maturation in the Weddell seal. *J. Dev. Physiol.* **9**, 477–493. (doi:10.1002/dev.420090510)
41. Pierrot-Deseilligny C, Milea D, Muri RM. 2004 Eye movement control by the cerebral cortex. *Curr. Opin. Neurol.* **17**, 17–25. (doi:10.1097/00019052-200402000-00005)
42. Langworthy OR, Hesser F, Kolb LC. 1938 A physiological study of the cerebral cortex of the hair seal (*Phona vitulina*). *J. Comp. Neurol.* **69**, 351–369. (doi:10.1002/cne.900690302)
43. Brown TA, Joanisse MA, Gati JS, Hughes SM, Nixon PL, Menon RV, Lomber SG. 2013 Characterization of the blood-oxygen level-dependant (BOLD) response in cat auditory cortex using high-field fMRI. *Neuroimage* **64**, 458–465. (doi:10.1016/j.neuroimage.2012.09.034)
44. Gábor A, Gácsi M, Szabó D, Miklósi Á, Kubinyi E, Andics A. 2020 Multilevel fMRI adaptation for spokes word processing in the awake dog brain. *Sci. Rep.* **10**, 11968. (doi:10.1038/s41598-020-68821-6)
45. Alderson AM, Diamantopoulos E, Downman CBB. 1960 Auditory cortex of the seal (*Phoca vitulina*). *J. Anat.* **94**, 506–511.
46. Ladygina TF, Popov VV, Supin AY. 1985 Topical organization of somatic projections in the fur seal cerebral cortex. *Neurophysiology* **17**, 246–252. (doi:10.1007/BF01052461)
47. Brigadoi S, Ceccherini L, Cutini S, Scarpa F, Scatturin P, Selb J, Gagnon L, Boas DA, Cooper RJ. 2014 Motion artifacts in functional near-infrared spectroscopy: a comparison of motion correction techniques applied to real cognitive data. *Neuroimage* **85**, 181–191. (doi:10.1016/j.neuroimage.2013.04.082)
48. Cooper RJ, Selb J, Gagnon L, Phillip D, Schytz HW, Iversen HK, Ashina MA, Boas DA. 2012 A systematic comparison of motion artifact correction techniques for functional near-infrared spectroscopy. *Front. Neurosci.* **6**, 1–10. (doi:10.3389/fnins.2012.00147)
49. Huppert TJ. 2016 Commentary on the statistical properties of noise and its implication on general linear models in functional near-infrared spectroscopy. *Neurophotonics* **3**, 010401. (doi:10.1117/1.nph.3.1.010401)
50. Thompson D, Hammond PS, Nicholas KS, Fedak MA. 1991 Movements, diving and foraging behaviour of grey seals (*Halichoerus grypus*). *J. Zool. Lond.* **224**, 223–232. (doi:10.1111/j.1469-7998.1991.tb04801.x)
51. Ruesch A, Yang J, Schmitt S, Acharya D, Smith MA, Kainerstorfer JM. 2020 Estimating intracranial pressure using pulsatile cerebral blood flow measured with diffuse correlation spectroscopy. *Biomed. Opt. Exp.* **11**, 1462–1476. (doi:10.1364/BOE.386612)
52. Massen J, Colier W, Hopman J, Liem D, de Korte C. 2009 A method to calculate arterial and venous saturation from near infrared spectroscopy. *Adv. Exp. Med. Biol.* **645**, 135–140. (doi:10.1007/978-0-387-85998-9_21)
53. McKnight JC *et al.* 2021 When the human brain goes diving: using near-infrared spectroscopy to measure cerebral and systemic cardiovascular responses to deep, breath-hold diving in elite freedivers. *Phil. Trans. R. Soc. B* **376**, 20200349. (doi:10.1098/rstb.2020.0349)
54. Russell DJF, Hastie GD, Thompson D, Janik VM, Hammond PS, Scott-Hayward LAS, Matthiopoulos J, Jones EL, McConnell BJ. 2016 Avoidance of wind farms by harbour seals is limited to pile driving activities. *J. Appl. Ecol.* **53**, 1642–1652. (doi:10.1111/1365-2664.12678)
55. Goldbogen JA *et al.* 2013 Blue whales respond to simulated mid-frequency military sonar. *Proc. R. Soc. B.* **280**, 20130657. (doi:10.1098/rspb.2013.0657)
56. Virtanen J, Noponen T, Kotilahti K, Virtanen J, Ilmoniemi RJ. 2011 Accelerometer-based method for correcting signal baseline changes caused by motion artifacts in medical near-infrared spectroscopy. *J. Biomed. Opt.* **16**, 087005. (doi:10.1117/1.3606576)
57. Haeussinger FB, Heinzel S, Hahn T, Schecklmann M, Ehlis A-C, Fallgatter AJ. 2011 Simulation of near-infrared light absorption considering individual head and prefrontal cortex anatomy: implications for optical neuroimaging. *PLoS ONE* **6**, E26377. (doi:10.1371/journal.pone.0026377)
58. Tift MS, Ponganis PJ, Crocker DE. 2014 Elevated carboxyhemoglobin in a marine mammal, the northern elephant seal. *J. Exp. Biol.* **217**, 1752–1757. (doi:10.1242/jeb.100677)
59. Rosen DAS, Gerlinsky CG, Trites AW. 2018 Telemetry tags increase the costs of swimming in northern fur seals, *Callorhinus ursinus*. *Mar. Mam. Sci.* **34**, 385–402. (doi:10.1111/mms.12460)